ORIGINAL ARTICLE

Proteomic Analysis of Human Breast Cancer MCF-7 Cells to Identify Cellular Targets of the Anticancer Pigment OR3 from *Streptomyces coelicolor* JUACT03

Somasekhara D[1] · Manjunath Dammalli[2] · Varalakshmi Kilingar Nadumane[1]

Abstract

Search for ideal compounds with known pathways of anticancer mechanism is still a priority research focus for cancer, as it continues to be a major health challenge across the globe. Hence, in the present study, anticancer potential of a yellow pigment fraction, OR3, isolated from *Streptomyces coelicolor* JUACT03 was assessed on the breast cancer cell line MCF-7. TLC-fractionated OR3 pigment was subjected to HPLC and GC–MS analysis for characterization and identification of the bioactive component. MCF-7 cells were treated with IC_{50} concentration of OR3 and the molecular alterations were analyzed using mass spectrometry-based quantitative proteomic analysis. Bioinformatics tools such as STRING analysis and Ingenuity Pathway Analysis were performed to analyze proteomics data and to identify dysregulated signaling pathways. As per our obtained data, OR3 treatment decreased cell proliferation and induced apoptotic cell death due to significant dysregulation of protein expressions in MCF-7 cells. Altered expression included the ribosomal, mRNA processing and vesicle-mediated transport proteins as a result of OR3 treatment. Downregulation of MAPK proteins, NFkB, and estradiol signaling was identified in OR3-treated MCF-7 cells. Mainly eIF2, mTOR, and eIF4 signaling pathways were altered in OR3-treated cells. GC–MS data indicated the presence of novel compounds in OR3 fraction. It can be concluded that OR3 exhibits potent anticancer activity on the breast cancer cells mainly through altering the expression and affecting the signaling proteins which are involved in different cell proliferation/apoptotic pathways thereby causing inhibition of cancer cell proliferation, survival and metastasis.

Keywords Pigment · *Streptomyces coelicolor* · Anticancer · Proteomics · GC–MS · String analysis · Ingenuity Pathway · Signaling pathways

✉ Varalakshmi Kilingar Nadumane
  kn.varalakshmi@jainuniversity.ac.in

  Somasekhara D
  d.somasekhara@jainuniversity.ac.in

  Manjunath Dammalli
  manjunathdammalli@sit.ac.in

1 Department of Biotechnology, School of Sciences, JAIN (Deemed-to-Be-University), Bangalore 560078, Karnataka, India

2 Department of Biotechnology, Siddaganga Institute of Technology, Tumakuru 572103, India

Introduction

Cancer remains a global health issue even today, despite rapid advancements in its detection or treatment modalities. The most common type of cancer among women is breast cancer, being the primary cause of cancer deaths and causing the most disability adjusted life years (DALYs) lost around the world (1.7 million breast cancer cases and 0.53 million deaths) [1, 2]. CONCORD-3 in 2018 reported a 5-year breast-cancer survival rates that was more than 90% in the USA, while it was only 66% in India as of 2014 data [3, 4].

Human cancer cells undergo various cellular and molecular alterations due to specific genetic, environmental causes leading to impaired signaling mechanisms and their uncontrollable multiplication [5]. Cancer cells develop resistance to many chemotherapeutic drugs, and hence pose a great challenge for therapeutic approaches. The search of novel drugs that overcome these problems by regulating signaling pathways is a priority goal for cancer researchers across the world [6]. In this respect, natural products (NPs) isolated from plants and microorganisms have made significant contribution towards cancer drug discovery and many compounds from natural sources have entered clinical trials [7, 8].

Streptomyces sp., an Actinomycetes group of microbes, have contributed several NPs/ secondary metabolites having antioxidant, anticancer, antimicrobial, and immunosuppressive properties. Some anticancer drugs produced by *Streptomyces* are bleomycin, dactinomycin, mitomycin C, and doxorubicin. Based on such previous discoveries from *Streptomyces*, this genus has emerged as a major target to explore novel anticancer compounds [9, 10].

Though many natural compounds were analyzed for their anticancer potential, their mechanism of action were not investigated extensively with respect to their molecular targets within a cancer cell. Precise cancer treatment is feasible if we have a thorough understanding of the primary targets of the anticancer compound within a cancer cell. The intervention of proteomics and artificial intelligence (AI) to analyze the effects of a compound on the differentially expressed proteins of signaling pathways within a cancer cell would greatly improve our understanding about the cellular targets of anticancer drugs [11]. Recently, the use of artificial intelligence as a tool to discover novel anticancer compounds from natural resources and to understand their mechanism of action has gained greater significance [12].

In the present study, we analyzed the effects of a yellow pigment (OR3) from *Streptomyces coelicolor* JUACT03, previously isolated and maintained in our lab, on MCF-7 breast cancer cell line using LC–MS/MS whole proteomic approach. Using this proteomics data, we analyzed different aspects like protein–protein interaction, gene ontology studies, pathway analysis, signaling proteins, and upstream regulators to understand the possible anticancer mechanism of OR3 in MCF-7 cells.

Materials and Methods

Extraction of Pigment from Streptomyces coelicolor Isolate

A promising isolate of Actiomycete was identified as *Streptomyces coelicolor* by 16 s rRNA sequencing and maintained in our lab. The sequence was deposited in GenBank with the accession number NR_025870.2. A distance matrix tree was constructed using the

Jukes-Cantor corrected distance model and the topology of the phylogenetic tree was built by using Weighted neighbor-joining method [13]. From this isolate, the orange pigment was extracted as previously reported [14].

Cell lines Used

The breast cancer MCF-7 cell line used in the present study was procured from the National Centre for Cell Sciences (NCCS), Pune, India. These cells were maintained in minimal essential medium (MEM, HiMedia) supplemented with 10% fetal bovine serum (FBS, HiMedia) The cells were incubated at 37 °C with 5% CO_2 in a humidified incubator.

Screening for Anticancer Activities

The MCF-7 cell line was cultured in 96-well microtiter plates and incubated for 24 h. The sample was added at varying concentrations to the cells in the plates and incubated for 24, 48, and 72 h. After the incubation period, 10 µl of 5 mg/ml MTT dye was added to the wells and the plates were incubated for 3 h at 37 °C in a dark chamber. DMSO (100 µl) was added to the wells to dissolve the formazan crystals formed and the absorbance was recorded at 540 nm, using an ELISA plate reader (Lisa Plus) [15]. IC_{50} values were determined from the dose–response curves. The experiment was conducted in triplicates.

Partial Purification of the Pigment

Pre-coated silica TLC sheets (60 F 254, Merck) were used to fractionate the pigment. The plates were activated at 110 °C for 15 min. The pigment extract (5 mg/ml) was dissolved in methanol and approximately 20 µl of the sample was loaded onto the TLC plate. Methanol and hexane in the ratio 7:3 was used as the solvent system to fractionate the extract. From the developed TLC sheet, each band was scraped, extracted with methanol, and centrifuged at 10,000 rpm for 10 min [14]. The supernatant was evaporated at room temperature (28–30 °C) to collect the purified fractions. The partially purified fractions were screened for their cytotoxic activity by performing the 3-(4,5-dimethylthiazol-2-yl)-2,5-diphenyl tetrazolium bromide MTT assay against the cancer cell lines. The fraction with highest cytotoxic activity was selected for further studies.

HPLC Purification of OR3 Fraction

The partially purified fraction OR3 was purified by running the sample in a semi-preparative HPLC (LC-20AD plus Detector, Shimadzu, Japan) connected to a system with LabSolutions software. The pumps (pump A and pump B) were used to pass the pressurized liquid solvent (water:methanol) along with sample. Pump A was always maintained as water (default) and pump B was set as Methanol.

Gas Chromatography-Mass Spectrometry (GC–MS) Analysis

The HPLC-purified yellow pigment (OR3) fraction was analyzed for the presence of different volatile compounds by gas chromatography-mass spectroscopy (GC–MS) at "The South India Textile Research Association (SITRA)," Coimbatore, Tamil Nadu, India. GC

analysis was performed using a GC MS/MS (Model; Agilent Technologies GC: 8890; MS: 7000D GC/TQ) equipped with a HP 5MS Ultra inert fused silica capillary column (30 m length × outside diameter 250 µm × internal diameter 0.25 µm). Helium was used as the carrier gas at a constant flow rate of 1.516 ml/min and the sample injected was 2 µl; injector temperature was 250 °C; ion source temperature was 280 °C. The oven temperature was programmed from 80° C for 2 min, 200 °C for 2 min at the rate of 15 °C/min, 240 °C for 2 min at the rate of 4 °C/min, and finally raised to 280 °C for 15 min at 15 °C/min; total run time was 31.66 min. Transfer line temperature was kept at 250 °C. The relative percentage of each extract constituent was expressed as percentage with peak area normalization.

Identification of Components

Identification was based on the molecular structure, molecular mass, and calculated fragments. Interpretation on mass spectrum of GC–MS was through the database of the National Institute of Standards and Technology (NIST). The name, molecular weight, and structure of the components of the test materials were ascertained. The relative percentage of each component was calculated by comparing its average peak area to the total area. The spectrum of the unknown component was compared with the spectrum of the component stored in the NIST library version NIST MS search V.2.3: 2017.

Treatment of MCF-7 Cells for Proteomics

MCF-7 cells (2.6×10^6) were seeded into 75 cm^2 culture flasks with supplemented culture medium. After 24 h, cells were treated with IC$_{50}$ concentration of TLC-purified yellow pigment and left for 12 h. The negative control group was treated with the same amount of PBS with 10% DMSO. Experimental procedures were performed at least in triplicate. After 12 h, cells were harvested.

Sample Preparation for LC–MS/MS

Cells were lysed in lysis buffer (2% SDS in 50 mM triethylammonium bicarbonate), and were subjected to five cycles of sonication for 30 s and 20% amplitude with an interval of 5 s each in Branson 450 Digital Sonifier (Marshall Scientific, Hampton, NH, USA). The lysates were subjected to centrifugation for 10 min at 14,000 rpm and the clear supernatant was collected and aliquoted. One aliquot was used for protein estimation using BCA (bicinchoninic acid) assay (Thermo Scientific) and the other aliquot was stored at − 80 °C till further analysis [16, 17]. Equal amount of protein from controls C1, C2, and C3 and OR3-treated T1, T2, and T3 was precipitated using ice-cold acetone. Among the controls, C1 was taken and T1, T2, and T3 were considered separate samples and compared with the C1. In-solution digestion and fractionation were performed as described previously [18, 19]. In brief, 500 µg of protein was subjected to reduction using 100 mM DTT and alkylation using 10 mM iodoacetamide, followed by digestion using trypsin (Promega, Madison, WI. Cat #: V5111) for 16 h at 37 °C. Digested peptides were purified using Sep-Pak C$_{18}$ material and vacuum dried in SpeedVac Vacuum Concentrators (Thermo Scientific) according to the methodology reported previously [20].

Fractionation

The tryptic peptides cleaned using Sep-Pak C_{18} material were subjected to stage tip-based SCX (strong cation-exchange) fractionation to generate 12 fractions, as described previously. Briefly, stage tip was packed using SCX disks and activated using ACN. Vacuum dried peptides were reconstituted in loading buffer (1% trifluoroacetic acid (TFA)) and loaded on the disk and washed with 0.2% TFA. After washing, the peptides were fractionated by different gradients of ammonium acetate (50 mM, 75 mM, 125 mM, 200 mM, and 300 mM) with 20 mM CAN and 0.5% formic acid as described earlier [21]. A total of 12 fractions were collected, vacuum dried, and stored in −80 °C until LC–MS/MS analysis.

Mass Spectrometry Data Acquisition

All the 12 fractions were analyzed on an Orbitrap Fusion Tribrid mass spectrometer (Thermo Electron, Bremen, Germany) interfaced with Easy-nLC II nanoflow liquid chromatography system (Thermo Scientific, Odense, Denmark). A total of 12 fractions were analyzed on mass spectrometry. Briefly, peptides from each fraction were reconstituted in solvent A and separated on an analytical column (75 μm×50 cm), LC (liquid chromatography, C_{18}) at a flow rate of 280 NL/min using a step gradient of 8–22% solvent B (0.1% formic acid in 90% acetonitrile) for first 70 min, followed by 22–35% up to 103 min. The total run time was set to 120 min. The mass spectrometer was operated in a data-dependent acquisition (DDA) mode. A survey full scan MS (from m/z 350–1600) was acquired in the Orbitrap at a resolution of 120,000 at 200 m/z. The AGC (automatic gain control) target for MS1 was set as 4×10^5 and ion filling time set for 50 ms. The most intense ions with charge state ≥2 was isolated and fragmented using HCD (higher collision dissociation) fragmentation with 34% normalized collision energy and detected at a mass resolution of 50,000 at 200 m/z. The AGC target for MS/MS was set as 1×10^5 and ion filling time set 100 ms dynamic exclusion was set for 30 s [16].

Mass Spectrometry Data Analysis

The mass spectrometry raw data were searched using SEQUEST and MS Amanda search engines with Proteome Discoverer 2.1 (Thermo Fisher Scientific). For label-free quantification, Minora Feature Detector node in the processing workflow of the Proteome Discoverer and the Precursor Ions Quantifier node and the Feature Mapper in the consensus workflow were used. The data was searched against the Human RefSeq 89 database. "Minora Feature Detector" node performs an efficient MS1-based quantification by detecting, aligning, and matching peaks across LC/MS runs, and by mapping them to the corresponding peptide sequences identified by MS2. The search parameter used as carbamidomethylation of cysteine residues as a fixed modification. Oxidation of methionine was selected as dynamic modifications. Trypsin was set as the protease and a maximum of two missed cleavage were allowed. Precursor mass tolerance was set to 10 ppm, and a fragment mass tolerance of 0.05 Da was allowed. All peptide-spectrum matches (PSM) were identified at a 1% false-discovery rate (FDR) as reported earlier [22]. Protein quantification was carried out according to "LFQ" (normalized intensity) value. PD provided for each quantified protein the height of the most abundant peak at the apex of the chromatographic profile ("intensity") and the integrated peak area ("area"). A normalization step (or no) was applied for the quantitative values based on the total peptide intensity of the samples. The quantified value reported for a given protein is actually the sum of the quantification values of all peptides belonging to that protein [23].

Bioinformatics Analysis of the Identified Proteins

Bioinformatics analysis of the identified proteins was carried out as reported previously [24, 25]. Briefly, the differentially expressed proteins were subjected to network analysis using STRING database (https://string-db.org). PANTHER database (http://www.panth erdb.org/) was used to perform Gene Ontology analysis for an inventory of the proteins making up the individual organelles and associated biological processes. Analysis of altered molecular pathways, canonical pathways, and prediction of upstream regulators was performed using Ingenuity Pathway Analysis (IPA) (https://ingenuity.com/products/ipa).

Statistical Analysis

All the experiments were carried out in triplicates. Results were calculated as mean ± standard error. Statistical significance was calculated using one-way analysis of variance (ANOVA) using the GraphPad Prism 6.0 software. Sample means were compared using Duncan's multiple range test (DMRT). A significance level of $P < 0.05$ was employed to determine a significant difference between the control and the treated samples.

Results
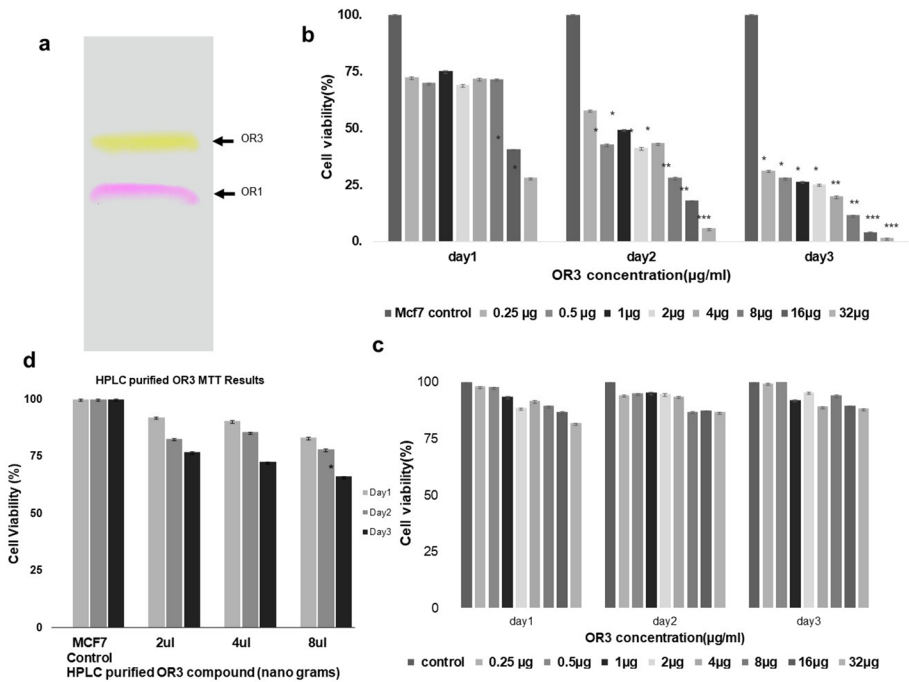
Identification of the Isolate

The isolate which showed potent anticancer activity on and MCF-7 cancer cell line was selected for the study and was identified as *Streptomyces coelicolor* JUACT03 by molecular methods. The sequence was deposited in GenBank with the accession no. NR_116633.1.

Thin-Layer Chromatography (TLC) and HPLC for Pigment Fractionation

The methanol extracted pigment from *Streptomyces coelicolor* was fractionated by TLC. We used methanol/hexane in the ratio of 7:3 for fractionation and the separated 3 fractions were named OR1, OR2 (detectable under UV light), and OR3 (Fig. 1a). The Rf values were noted as 0.77, 0.86, and 0.90, respectively. All fractions were tested for their cytotoxicity on MCF-7 cell line through MTT assay. The third fraction, which was yellow in color (named as OR3), exhibited highest cytotoxicity (results not shown) among the tested fractions. This OR3 fraction was subjected to HPLC for purification, which resulted in one single peak eluting out at RT 5.47 min (Supplementary File. S1Aa). This major fraction was collected by preparative HPLC and was further subjected to GC–MS analysis.

GC–MS Analysis

GC–MS analysis of the HPLC-purified OR3 fraction resulted in identification of 113 compounds and chromatogram showed five major peaks at different retention times (RT) (Supplementary File. S1Ab) and each compound is exhibiting difference in compound area. The mass spectral analysis of the major peak at RT 3.1134 min corresponds to the compound 1,3,5,7-tetroxane, peak at RT 3.6040 min corresponds to 1-phenyl-1-decanol, peak at RT

Fig. 1 **a** TLC fractionation of orange pigment extract from *Streptomyces coelicolor*. The arrows indicate the pigment fractions. OR3-yellow fraction and OR1-pink fraction. **b** The effect of OR3 fraction (0.25, 0.5, 1.0, 2.0, 4.0, 8.0, 16, and 32 µg/ml) on MCF-7 at 24, 48, and 72 h. **c** The effect of OR3 fraction (0.25, 0.5, 1.0, 2.0, 4.0, 8.0, 16, and 32 µg/ml) on lymphocytes at 24, 48, and 72 h. **d** Effect of HPLC eluted fraction on MCF-7 cells at 24, 48, and 72 h. The level of significance is indicated as *$P < 0.05$, **$P < 0.005$, and ***$P < 0.0001$ in comparison to the untreated control

3.7182 min corresponds to tetramethyl silicate, and the peak at RT 11.7705 min corresponds to cyclopentasiloxane, decamethyl- with a match factor of 72.7% (Supplementary File. 1B). The compound cyclopentasiloxane decamethyl- was reported earlier for antioxidant, antimicrobial, and antibacterial activities, though not for anticancer activity [26].

Cytotoxicity Analysis

OR3 fraction was further tested at 0.25, 0.5,1.0, 2.0, 4.0, 8.0, 16.0, and 32.0 µg/ml concentrations on MCF-7 cells for the treatment periods of 24, 48, and 72 h. Percentage viability of MCF-7 cells treated with OR3 (32 µg/ml) was 28% after a treatment period of 24 h which reduced further to 1.5% after 72 h of treatment (Fig. 1b). IC_{50} value of OR3 was calculated as 12.49 µg/ml for MCF7 cell line from the dose response curve. The cytotoxic effect was found to be significant. Treatment of OR3 at the same concentration (32 µg/ml) to normal healthy lymphocytes did not cause any significant change in the cell viability even after 48 or 72 h (Fig. 1c). Here, the percentage viability was ranging between 81 and 88%. Furthermore, the HPLC purified fraction was tested at different dilutions (2–8 µl) on MCF-7 cells for 24, 48, and 72 h. This fraction had demonstrated antiproliferative effects (Fig. 1d), thus confirming OR3's effectiveness for anticancer application studies.

OR3 Treatment Results in Proteomic Alterations in MCF7 Cells

We observed OR3 pigment as to have profound cytotoxic effects on the breast cancer MCF-7 cells. As the anticancer effect of the partially purified OR3 was significantly higher than the HPLC-purified fraction, OR3 was chosen for further proteomics studies on MCF-7. To understand the molecular mechanisms of antiproliferative effects of OR3, we performed mass spectrometry-based proteomic analysis of MCF-7 cells treated with OR3 along with untreated cells. Proteomic data showed 3009 non-redundant proteins in two conditions. In OR3-treated MCF-7 control, we observed overexpression of 528 proteins (17%), downregulation of 399 proteins (13%), and remaining proteins as unaltered (Fig. 2a). This MS proteomics data was deposited to the ProteomeXchange Consortium having the dataset identifier PXD032999. We considered a fold change cutoff of twofold and $P \leq 0.05$ to filter proteins for further analysis.

OR3 pigment caused characteristic molecular alterations in MCF-7 cells as per mass spectrometry analysis which indicated dysregulation of various proteins in treated cells. To further analyze the biological functions affected by altered proteins, we used bioinformatics tools, such as network analysis, gene ontology enrichment study, and pathway analysis. To predict protein–protein interactions among the dysregulated proteins, we performed network analysis using STRING database (https://string-db.org). As shown in the results of network analysis, proteins involved in vesicle-mediated transport,
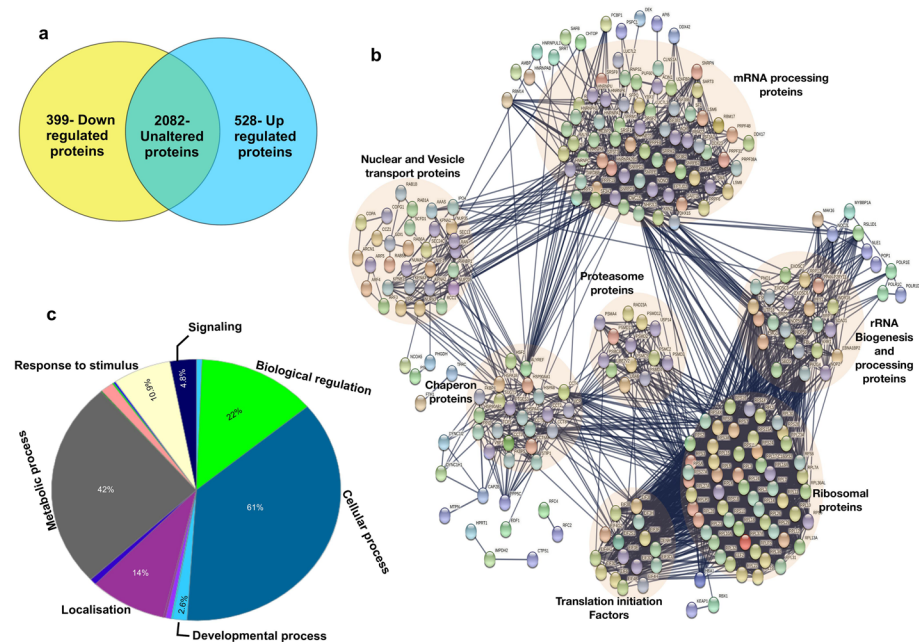

Fig. 2 a Identified proteins by LC–MS/MS. **b** Interaction network analysis: OR3-treated MCF-7 cells showed distinct molecular alterations. STRING interaction network depicts the association among the proteins. Circled balls are representing individual protein. Circled proteins are majorly involved in ribosomal, mRNA processing, rRNA processing, translation initiation factors, protein transport and processing. **c** Gene Ontology analysis: a pie chart depicting the dysregulated proteins involved in biological processes

ribosomal, rRNA processing, chaperon, proteasome, translation initiation factors, nuclear transport, and mRNA processing were majorly affected by OR3 in MCF-7 cells (Fig. 2b).

The PANTHER and HPRD-based Gene Ontology (GO) studies of the 927 dysregulated proteins indicated that majority of these proteins are involved in cellular processes (61%), metabolic process (42%), localization (14%), biological regulation (2.2%), response to stimulus (10.9%), developmental process (2.6%), and signaling (4.8%). The details of the GO analysis are represented in Fig. 2c.

OR3 Treatment Affects EIF2, EIF4, and mTOR Signaling

Ingenuity Pathway Analysis was used to analyze alteration of canonical pathways using a combination of over expressed and down regulated proteins as input. Our results revealed that, among the various canonical pathways affected in OR3 treated breast cancer cells, eIF2 signaling was the most predominant altered pathway (Fig. 3). Further analysis of these results indicated that 67 of the differentially expressed proteins are associated with the eIF2 pathway. eIF4 and mTOR signaling were also significantly affected in OR3 treated MCF-7 cells. Downregulated proteins in these pathways mainly belong to MAPK (mitogen activated protein kinases), translation initiation factors, and ribosomal proteins (Fig. 4 and Table 1).

Possible Upstream Regulator and Signaling Analysis

The results of the current study revealed that estradiol is a possible upstream regulator and ESR1, ESR2 and MYC proteins are downstream of estradiol signaling in breast cancer. One hundred thirty-six proteins, which are targets of estradiol signaling, are downregulated due to OR3 treatment as per our results. Upregulation of ribosomal proteins RPL5, RPL11, and RPS14 leads to the downregulation of MYC protein (Fig. 5a). Downregulated proteins mainly belong to MAPK proteins. Vesicle-mediated
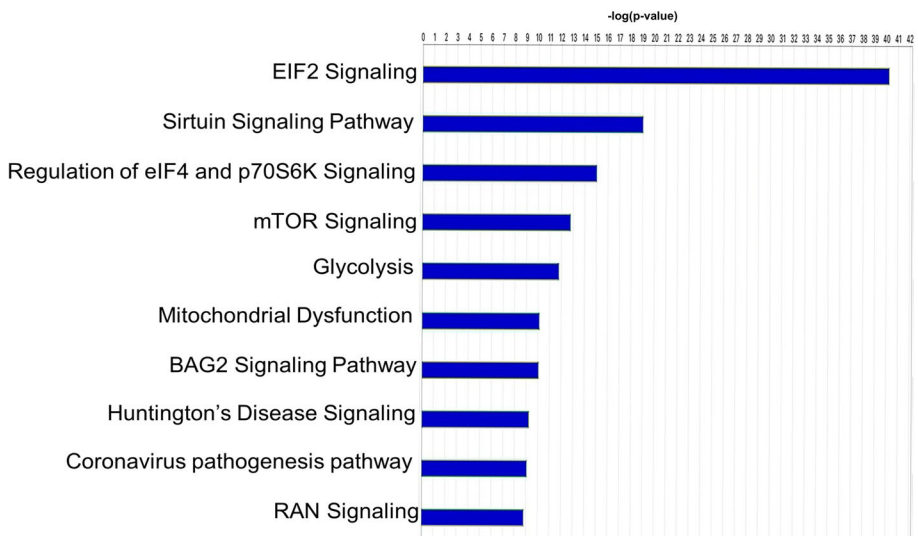

Fig. 3 Altered canonical pathways in OR3-treated MCF-7 cells
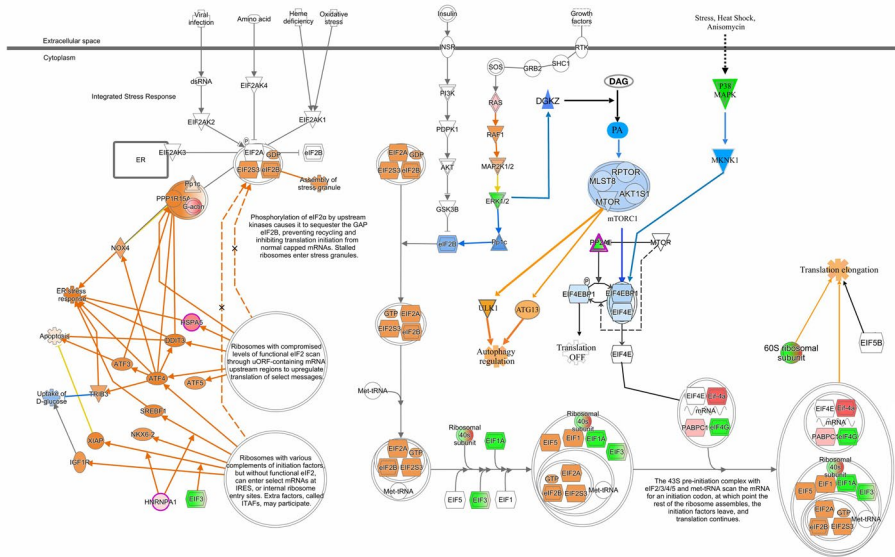
Fig. 4 OR3 treatment on MCF-7 cells affects eIF2, mTOR, and eIF4 signaling. Ingenuity pathway analysis of proteins significantly dysregulated ($P \leq 0.05$) in OR3-treated MCF-7/control MCF-7 cells. The signaling network of EIF2, mTOR, and EIF4 pathway based on differential expression of molecules upon OR3 treatment on MCF-7 cells

Table 1 Downregulated proteins in eIF2 pathway

Gene symbol	Description	Fold change in OR3 treated/ control
EIF1AY	Eukaryotic translation initiation factor 1A, Y-chromosomal	0.01
EIF3B	Eukaryotic translation initiation factor 3 subunit B	0.095
EIF3D	Eukaryotic translation initiation factor 3 subunit D	0.01
EIF3F	Eukaryotic translation initiation factor 3 subunit F	0.01
EIF3H	Eukaryotic translation initiation factor 3 subunit H	0.01
EIF3L	Eukaryotic translation initiation factor 3 subunit L	0.127
EIF4G2	Eukaryotic translation initiation factor 4 gamma 2	0.01
MAPK1	Mitogen-activated protein kinase 1	0.01
MAPK3	Mitogen-activated protein kinase 3	0.087
MAPK14	Mitogen-activated protein kinase 14	0.01
RPL14	60S ribosomal protein L14	0.067
RPL31	60S ribosomal protein L31	0.263
RPS24	40S ribosomal protein S24	0.119
RPL36AL	60S ribosomal protein L36a-like	0.01
RPL37A	60S ribosomal protein L37a	0.135
RPS10	40S ribosomal protein S10	0.187
RPS28	40S ribosomal protein S28	0.116
EIF4B	Eukaryotic translation initiation factor 4B	0.06
CDC42	Cell division control protein 42 homolog	0.831

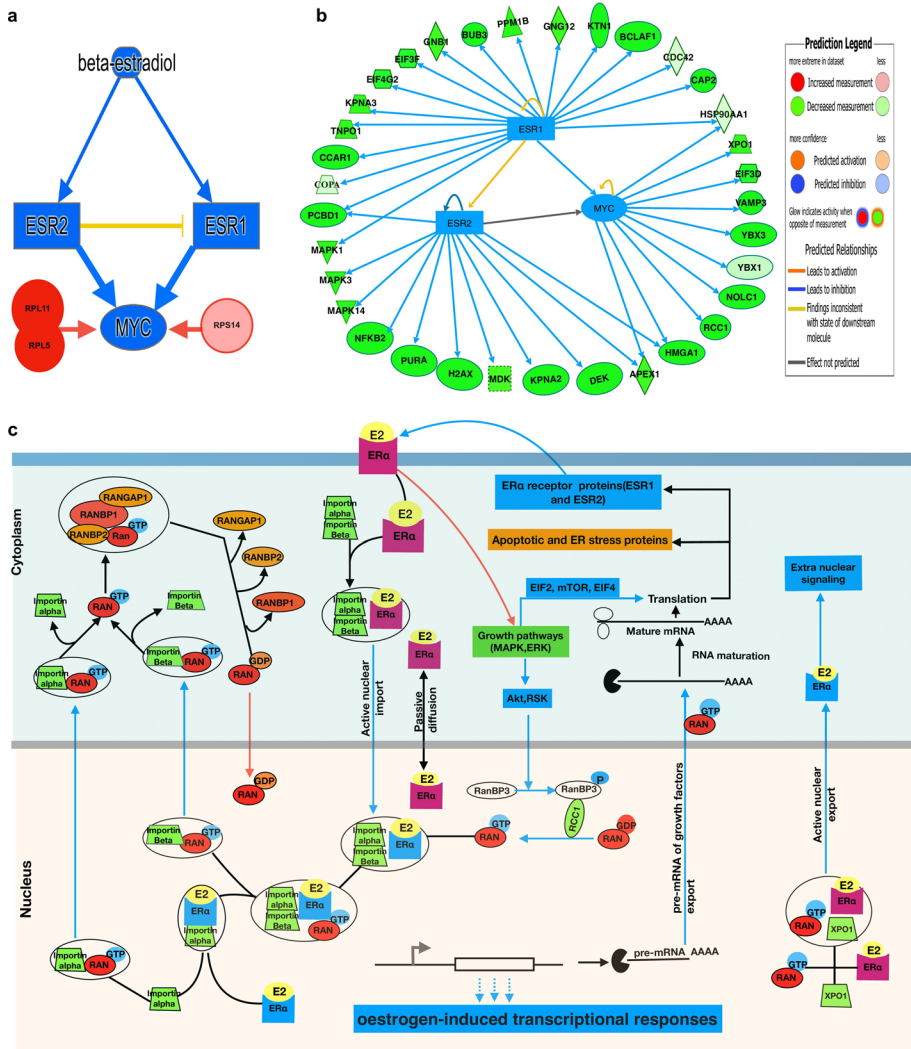**Fig. 5** **a** MYC protein downregulation through upregulation of ribosomal proteins and downregulation of estrogen receptor proteins. **b** In our data 136, ESR1, ESR2, and MYC target proteins were downregulated. Here showing some proteins belong to signaling proteins, transport proteins, and transcriptional factors. **c** RAN-mediated estrogen receptor shuttling pathway in OR3-treated MCF-7 cells

transport proteins, transcription factors required for cell cycle progression, and RAN-mediated importins and exportin proteins are downregulated in OR3-treated MCF-7 cells (Fig. 5b and c). Due to downregulation of RAN-mediated importin and exportins, estradiol signaling appears to be affected in OR3-treated MCF7 cells, which in turn might be affecting breast cancer cell proliferation and metastasis. The treatment of OR3 significantly downregulated/upregulated the expression of proteins in eIF2, mTOR, and eIF4 pathways (Fig. 6).
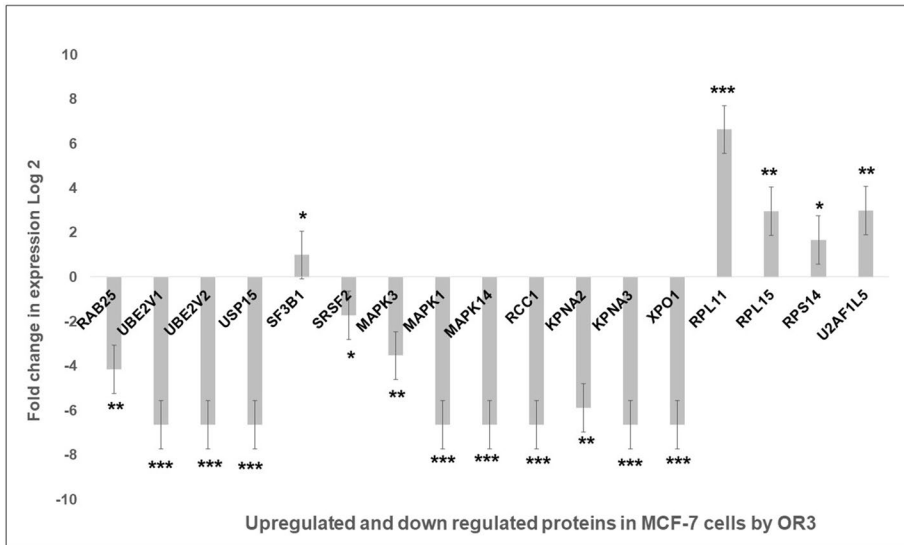
Fig. 6 The bar plot of downregulated and upregulated key proteins in MCF-7 cells by OR3. The OR3-induced changes at the protein level of eIF2, mTOR, and eIF4 pathways are shown here as bar graph in a Log2 scale. p value ranges from 0.01 to 0.00001

Discussion

The motive of this research work was to unravel the mechanism of action of a potent anticancer compound of microbial origin on the breast cancer cell line and to find out about the major signaling pathways affected. In the present work, *Streptomyces coelicolor* strain JUACT03 was selected as it demonstrated significant cytotoxic effects to the cancer cell lines. The yellow pigment (OR3), resulted by TLC fractionation of the crude pigment extract, was highly promising in inhibiting the proliferation of MCF-7 cancer cells in a concentration-dependent manner. The OR3 pigment, with an IC_{50} value of 12.49 μg/ml, was found to have significant cytotoxic effects against MCF-7 cell line as compared to prior study reports on different anticancer pigments [27], besides not to have any significant cytotoxic effects on the normal healthy lymphocytes at the same treated concentrations, suggesting its specificity towards cancer cells. The HPLC-purified fraction was having lesser cytotoxic effects to MCF-7 cells as compared to the partially purified OR3, maybe due to the synergistic effects of other unknown/unidentified components in this. Hence, we proceeded with OR3 fraction for further studies regarding anticancer mechanism.

A full proteome approach and label-free LC–MS/MS were adopted to study the anticancer mechanism of OR3 on the breast cancer cells. Through network analysis of dysregulated proteins, it was found that many biological function-related proteins were altered in the OR3-treated MCF-7 cells such as ribosomal, protein translation, spliceosomal, RAN pathway, chaperons, and vesicle transport proteins.

Cancer has been linked to disruptions in vesicle trafficking regulation which controls important signaling proteins both inside and outside of the cell [12]. Some of the vesicle-associated proteins were found to be dysregulated in our study, including RAB protein family which was earlier reported with respect to cancers of the ovary and the

breast [28]. RAB25 was downregulated after OR3 treatment in our study indicating it as one of the means through which it inhibited the cancer cell proliferation.

Elevated amounts of chaperone proteins are linked to a variety of events such as insensitivity to growth-inhibitory signals, self-sufficiency in growth signals, greater replicative potential, and apoptosis avoidance [29]. According to reports, HSF1 gene is downregulated in multiple cancer types and is responsible for the production of numerous heat shock proteins [30]. Ubiquitin-conjugating enzyme E2 (UBE2) family members are ubiquitin-related enzymes, and a number of studies have indicated their involvement in cancer. According to our findings, UBE2V1 and UBE2V2 are downregulated, while they were previously reported as upregulated in numerous cancers [31, 32]. USP15 plays a key function in the stabilization of the MDM2 protein, which promotes cancer cell survival. Tumor cell apoptosis and antitumor T cell responses are boosted when USP15 expression is inhibited [33]. In our findings, we observed that USP15 is downregulated. Apoptosis might have resulted from the downregulation of USP15 in OR3-treated MCF-7 cells in the present study.

Defects in RPs (ribosomal proteins), rRNA processing, or ribosome assembly factors have been linked to cancer in numerous studies. Ribosomal proteins that are dysregulated perform a variety of activities, including reprogramming translation for cancer-promoting mRNAs, altering proteasome activity, metabolic rewiring, and exhibiting higher levels of oxidative DNA damage [34]. In our study, as per network pharmacology, RPL11, RPL5, and RPS14 proteins were found upregulated. Upregulation of these ribosomal proteins affects c-MYC gene transcription and directs c-MYC mRNA to be degraded by the RNA-induced silencing complex (RISC) [35–37]. As a result, the expression of c-MYC target genes is affected. Alterations in splicing events occur in all types of malignancies that are not found in normal tissues, and tumors have up to 30% more alternative splicing events than normal tissues. Alternatively, spliced mRNA isoforms in particular have an impact on a variety of cancer processes, including tumor development and invasion, cell proliferation, apoptosis, angiogenesis, and metabolism. According to previous reports, the genes SF3B1, U2AF1, and SRSF2 are linked to cancer progression. Splicing proteins SF3B6, SF3B1, and SRSF2 were found to be downregulated and splicing factors SF3B2 and U2AF1 are upregulated in our study [38]. These observations are confirming the anticancer activity of OR3.

According to canonical pathway analysis, the eIF2 pathway was majorly affected by 67 dysregulated proteins in our current study. When the GDP-GTP exchange activity of the eIF2 -subunit is affected by stress, translation initiation gets inhibited from normally capped mRNAs, resulting in halted ribosomes entering stress granules. Translation of particular mRNAs involved in stress recovery and apoptosis is aided by eIF2 deficiency [39].

The phosphatases and mitogen-activated protein kinase (MAPK) signaling pathways are primarily involved in translational regulation via phosphorylation and dephosphorylation of translational machinery components. Dysregulation of these proteins causes pathological diseases, such as cancer [40]. According to our findings, ERK 1/2 is downregulated, which suggests that PP1c phosphatase protein is also downregulated. PP1c protein enhances dephosphorylation of phosphorylated eIF2B complex in the cytoplasm [41]. mTOR signaling is projected to be downregulated as a result of ERK 1/2 downregulation based on our findings. Downregulation of ERK 1/2 is implicated to result in a decrease in DGK ZETA1 protein activity, affecting the conversion of diacylglycerol to phosphoric acid [42]. Phosphatidic acid deficiency affects mTOR signaling, which affects protein translation [43, 44]. According to our results, p38 MAPK is downregulated, which means MKNK1 protein activity is reduced, which leads to non-phosphorylated forms of 4E-BP1 and eIF4E, that affects translation.

We looked at downregulated proteins to see whether there were any upstream regulators affecting MCF-7 cell growth after treatment with OR3. Breast cancer cell lines with high estrogen receptor (ER) expression exert their effects on target cells via two subtypes of estrogen receptors. The small GTPase protein RAN coordinates intracellular distribution and equilibrium of estrogen receptors. RCC1, Importin-(KPNA, KPNA2, KPNA3), importin-(KPNB1), and exportin (XPO1) family proteins are involved in the import and export of numerous steroid hormone receptors between the cytoplasm and the nucleus, and their downregulation affects the RAN pathway [45]. According to our findings, 136 proteins were downregulated with target proteins for the transcription factors ESR1, ESR2, and MYC. The transcription factors ESR1 and ESR2 are primarily engaged in 17-estradiol signaling. ESR1 increases MYC expression in MCF-7 cells [46]. Extranuclear ligand 17-estradiol with estrogen receptor stimulates mitogen-activated MAPK/ERK or PI3K/AKT/mTOR complex, which activates protein synthesis necessary for cell proliferation, cell cycle progression, survival, angiogenesis, invasion, and migration in cancer cells [47]. The expression and activation of proteins of p38 and MAPK pathways are influenced by estradiol signaling [48, 49]. MAPK and mTOR pathways are influenced by the downregulation of estradiol pathway. All these reports suggest that OR3 treatment on MCF7 cells might have impacted protein translation pathways, eIF2, mTOR, and eIF4 by downregulating the major signaling pathways such as p38, MAPK, RAN, and the estrogen receptors, according to the obtained data in our current study.

From the current study, it can be concluded that the OR3 pigment from *S. coelicolor* has significant anticancer effects on the breast cancer cells via modifying the expression of key signaling proteins involved in tumorigenesis, tumor metastasis, and tumor progression. However, further in vivo studies on mice models are warranted to take this study to the clinical level and drug developmental studies.

Declarations

References

1. Duggan, C., Dvaladze, A., Rositch, A. F., Ginsburg, O., Yip, C. H., Susan Horton, S., Rodriguez, R. C., Eniu, A., Mutebi, M., Bourque, J. M., Masood, M. S., Saldana, K. U., Cabanes, A., Carlson, R. W., Gralow, J. R., & Anderson, B. O. (2020). The breast health global initiative 2018 global summit on improving breast healthcare through resource-stratified phased implementation: Methods and overview. *Cancer, 126*(10), 2339–2352. https://doi.org/10.1002/cncr.32891

2. Fitzmaurice, C., Akinyemiju, T. F., Lami, F. H., et al. (2018). Global, regional, and national cancer incidence, mortality, years of life lost, years lived with disability, and disability-adjusted life-years for 29 cancer groups, 1990 to 2016: A systematic analysis for the global burden of disease study. *JAMA Oncology, 4*(11), 1553–1568. https://doi.org/10.1001/jamaoncol.2018.2706

3. Allemani, C., Matsuda, T., Di Carlo, V., Harewood, R., Matz, M., Niksic, M., Bonaventure, A., Valkov, M., Johnson, C. J., Esteve, J., Ogunbiyi, O. J., Silva, G. A., Chen, W. Q., Eser, S., Engholm, G., Stiller, C. A., Monnereau, A., Woods, R. R., Visser, O., … MP. (2018). Global surveillance of trends in cancer survival 2000–14 (CONCORD-3): Analysis of individual records for 37 513 025 patients diagnosed with one of 18 cancers from 322 population-based registries in 71 countries. *Lancet, 391*(10125), 1023–1075. https://doi.org/10.1016/s0140-6736(17)33326-3

4. Siegel, R. L., Miller, K. D., & Jemal, A. (2020). Cancer statistics. *CA: A Cancer Journal for Clinicians, 70*(1), 7–30. https://doi.org/10.3322/caac.21590

5. Law, J. W. F., Law, L. N. S., Letchumanan, V., Tan, L.T.-H., Wong, S. H., Chan, K.-G., Ab Mutalib, N.-S., & Lee, L.-H. (2020). Anticancer drug discovery from microbial sources: The unique mangrove streptomycetes. *Molecules, 25*(22), 5365. https://doi.org/10.3390/molecules25225365

6. Berdy, J. (2005). Bioactive microbial metabolites. *Journal of Antibiotics, 58*(1), 1–26. https://doi.org/10.1038/ja.2005.1

7. Harvey, A., Edrada-Ebel, R., & Quinn, R. (2015). The re-emergence of natural products for drug discovery in the genomics era. *Nature Reviews. Drug Discovery, 14*, 111–129. https://doi.org/10.1038/nrd4510

8. Newman, D. J., & Cragg, G. M. (2012). Natural products as sources of new drugs over the 30 years from 1981 to 2010. *Journal of Natural Products., 75*(3), 311–335. https://doi.org/10.1021/np200906s

9. Solanki, R., Khanna, M., & Lal, R. (2008). Bioactive compounds from marine actinomycetes. *Indian J Microbiol., 48*(4), 410–431. https://doi.org/10.1007/2Fs12088-008-0052-z

10. Olano, C., Mendez, C., & Salas, J. A. (2009). Antitumor compounds from marine actinomycetes. *Marine Drugs, 7*(2), 210–248. https://doi.org/10.3390/md7020210

11. Huang, M., Lu, J. J., & Ding, J. (2021). Natural products in cancer therapy: Past, present and future. *Natural Products and Bioprospecting, 11*, 5–13. https://doi.org/10.1007/s13659-020-00293-7

12. Zhang, R., Li, X., Zhang, X., Qina, H., & Xiao, W. (2020). Machine learning approaches for elucidating the biological effects of natural products. *Natural Product Reports., 38*,. https://doi.org/10.1039/D0NP00043D

13. Bruno, W. J., Socci, N. D., & Halpern, A. L. (2000). Weighted neighbor joining: A likelihood-based approach to distance-based phylogeny reconstruction. *Molecular Biology and Evolution, 17*(1), 189–197. https://doi.org/10.1093/oxfordjournals.molbev.a026231

14. Prashanthi, K., Suryan, S., Varalakshmi, K. N. (2015). In vitro anticancer property of yellow pigment from Streptomyces griseoaurantiacus JUACT 01. *Brazilian Archives of Biology and Technology*, 58(6). https://doi.org/10.1590/S1516-89132015060271.

15. Mosmann, T. (1983). Rapid colourimetric assay for cellular growth and survival: Application to proliferation and cytotoxicity assays. *Journal of Immunological Methods, 65*(1–2), 55–63. https://doi.org/10.1016/0022-1759(83)90303-4

16. Gondkar, K., Sathe, G., Joshi, N., Nair, B., Pandey, A., & Kumar, P. (2021). Integrated proteomic and phosphoproteomics analysis of DKK3 signaling reveals activated kinase in the most aggressive gallbladder cancer. *Cells, 10*(3), 511. https://doi.org/10.3390/cells10030511

17. Babu, N., Patil, S., Mohan, S. V., Subbannayya, T., Advani, J., Datta, K. K., Rajagopalan, P., Bhat, F. A., Sidransky, D., Gowda, H., & Chatterjee, A. (2021). Signaling alterations in oral keratinocytes in response to shisha and crude tobacco extract. *Journal of Oral Pathology and Medicine, 50*(5), 459–469. https://doi.org/10.1111/jop.13154

18. Advani, J., Verma, R., Chatterjee, O., Balaya, R. D. A., Najar, M. A., Ravishankara, N., Suresh, S., Pachori, P. K., Gupta, U. D., Pinto, S. M., Chauhan, D. S., Tripathy, S. P., Gowda, H., & Keshava Prasad, T. S. (2019). Rise of clinical microbial proteogenomics: A multiomics approach to nontuberculous mycobacterium-The case of *Mycobacterium abscessus UC22*. *OMICS: A Journal of Integrative Biology, 23*(1), 1–16. https://doi.org/10.1089/omi.2018.0116

19. Wisniewski, J. R., Zougman, A., Nagaraj, N., & Mann, M. (2009). Universal sample preparation method for proteome analysis. *Nature Methods, 6*(5), 359–362. https://doi.org/10.1038/nmeth.1322

20. Nirujogi, R.S., Muthusamy, B,. Kim, M.S., Sathe, G.J., P.T.V., Lakshmi, P.T.V., Kovbasnjuk, O.N., Keshava Prasad, T.S., Wade, M.,Jabbour, R.E. (2017). Secretome analysis of diarrhea-inducing strains of Escherichia coli. *Proteomics*, 17(6). https://doi.org/10.1002/pmic.201600299.

21. Kulak, N., Pichler, G., Paron, I., Nagaraj, N., & Mann, M. (2014). Minimal, encapsulated proteomic-sample processing applied to copy-number estimation in eukaryotic cells. *Nature Methods, 11*, 319–324. https://doi.org/10.1038/nmeth.2834

22. Dammalli, M., Murthy, K. R., Pinto, S. M., Murthy, K. B., Nirujogi, R. S., Madugundu, A. K., Dey, G., Nair, B., Gowda, H., & Keshava Prasad, T. S. (2017). Toward postgenomics ophthalmology: A proteomic map of the human choroid-retinal pigment epithelium tissue. *OMICS: A Journal of Integrative Biology, 2*, 114–122. https://doi.org/10.1089/omi.2016.0170

23. Palomba, A., Abbondio, M., Fiorito, G., Uzzau, S., Pagnozzi, D., & Tanca, A. (2021). Comparative evaluation of MaxQuant and proteome discoverer MS1-based protein quantification tools. *Journal of Proteome Research, 20*(7), 3497–3507. https://doi.org/10.1021/acs.jproteome.1c00143

24. Dammalli, M., Dey, G., Madugundu, A. K., Kumar, M., Rodrigues, B., Gowda, H., Siddaiah, B. G., Mahadevan, A., Shankar, S. K., & Prasad, T. S. K. (2017). Proteomic analysis of the human olfactory bulb. *OMICS: A Journal of Integrative Biology, 21*(8), 440–453. https://doi.org/10.1089/omi.2017.0084

25. Kumar, C., & Mann, M. (2009). Bioinformatics analysis of mass spectrometry-based proteomics data sets. *FEBS Letters, 583*(11), 1703–1712. https://doi.org/10.1016/j.febslet.2009.03.035

26. Ismail, G. A., Gheda, S. F., Abo-Shady, A. M., & Abdel-Karim, O. H. (2020). In vitro potential activity of some seaweeds as antioxidants and inhibitors of diabetic enzymes. *Food Sci Technol, 40*(3), 681–691.

27. El-Naggar, N. A. and El-Ewasy, S. (2017). Bioproduction, characterization, anticancer and antioxidant activities of extracellular melanin pigment produced by newly isolated microbial cell factories *Streptomyces glaucescens* NEAE-H. *Scientific Report*, 7(42129). https://doi.org/10.1038/srep42129.

28. Cheng, K. W., Lahad, J. P., Kuo, W. L., Lapuk, A., Yamada, K., Auersperg, N., Liu, J., Smith-McCune, K., Lu, K. H., Fishman, D., Gray, J. W., & Mills, G. B. (2004). The RAB25 small GTPase determines aggressiveness of ovarian and breast cancers. *Nature Medicine, 10*(11), 1251–1256. https://doi.org/10.1038/nm1125

29. Calderwood, S. K., & Gong, J. (2016). Heat shock proteins promote cancer: It's a protection racket. *Trends in Biochemical Sciences, 41*(4), 311–323. https://doi.org/10.1016/j.tibs.2016.01.003

30. Wawrzynow, B., Zylicz, A., Zylicz, M. (2018). Chaperoning the guardian of the genome. The two-faced role of molecular chaperones in p53 tumor suppressor action. *Biochimica et Biophysica Acta (BBA)*, 1869(2), 161–174. https://doi.org/10.1016/j.bbcan.2017.12.004.

31. Lagadec, C., Vlashi, E., Bhuta, S., Lai, C., Mischel, P., Werner, M., Henke, M., & Pajonk, F. (2014). Tumor cells with low proteasome subunit expression predict overall survival in head and neck cancer patients. *BMC Cancer, 5*(14), 152. https://doi.org/10.1186/1471-2407-14-152

32. Donna, L. D., Lagadec, C., & Pajonk, F. (2012). Radioresistance of prostate cancer cells with low proteasome activity. *Prostate, 72*(8), 868–874. https://doi.org/10.1002/pros.21489

33. Zou, Q., Jin, J., Hu, H., Li, H. S., Romano, S., Xiao, Y., Nakaya, M., Zhou, X., Cheng, X., Yang, P., Lozano, G., Zhu, C., Watowich, S. S., Ullrich, S. E., & Sun, S. C. (2014). USP15 stabilizes MDM2 to mediate cancer-cell survival and inhibit antitumor T cell responses. *Nature Immunology, 15*, 562–570. https://doi.org/10.1038/ni.2885

34. Kampen, K. R., Sulima, S. O., Vereecke, S., & De Keersmaecker, K. (2020). Hallmarks of ribosomopathies. *Nucleic Acids Research, 48*(3), 1013–1028.

35. Dai, M. S., Sears, R., & Lu, H. (2007). Feedback regulation of c-Myc by ribosomal protein L11. *Cell Cycle, 6*(22), 2735–2741. https://doi.org/10.4161/cc.6.22.4895

36. Liao, J. M., Zhou, X., Gatignol, A., & Lu, H. (2014). Ribosomal proteins L5 and L11 co-operatively inactivate c-Myc via RNA-induced silencing complex. *Oncogene, 33*(41), 4916–4923. https://doi.org/10.1038/onc.2013.430

37. Zhou, X., Hao, Q., Liao, J. M., Liao, P., & Lu, H. (2013). Ribosomal protein S14 negatively regulates c-Myc activity. *Journal of Biological Chemistry, 288*(30), 21793–21801. https://doi.org/10.1074/jbc.m112.445122

38. Desterro, J., Bak-Gordon, P., & Carmo-Fonseca, M. (2020). Targeting mRNA processing as an anticancer strategy. *Nature Reviews. Drug Discovery, 19*, 112–129. https://doi.org/10.1038/s41573-019-0042-3

39. Shrestha, N., Bahnan, W., Wiley, D. J., Barber, G., Fields, K. A., & Schesser, K. (2012). Eukaryotic initiation factor 2 (eIF2) signaling regulates proinflammatory cytokine expression and bacterial invasion. *Journal of Biological Chemistry, 287*(34), 28738–28744. https://doi.org/10.1074/jbc.M112.375915

40. Hinnebusch, A. G., Ivanov, I. P., & Sonenberg, N. (2016). Translational control by 5'-untranslated regions of eukaryotic mRNAs. *Science, 352*(6292), 1413–1416. https://doi.org/10.1126/science.aad9868

41. Quevedo, C., Salinas, M., & Alcázar, A. (2003). Initiation factor 2B activity is regulated by protein phosphatase 1, which is activated by the mitogen-activated protein kinase-dependent pathway in insulin-like growth factor 1-stimulated neuronal cells. *Journal of Biological Chemistry, 278*(19), 16579–16586. https://doi.org/10.1074/jbc.m212936200

42. Avila-Flores, A., Santos, T., Rincon, E., & Merida, I. (2005). Modulation of the mammalian target of rapamycin pathway by diacylglycerol kinase-produced phosphatidic acid. *Journal of Biological Chemistry, 280*(11), 10091–10099. https://doi.org/10.1074/jbc.m412296200

43. Liu, K., Xue, B., Bai, G., & Zhang, W. (2021). Downregulation of Diacylglycerol kinase zeta (DGKZ) suppresses tumorigenesis and progression of cervical cancer by facilitating cell apoptosis and cell cycle arrest. *Bioengineered, 12*(1), 1517–1529. https://doi.org/10.1080/21655979.2021.1918505

44. Roux, P. P., & Topisirovic, I. (2018). Signaling pathways involved in the regulation of mRNA translation. *Molecular and Cellular Biology, 38*(12), e00070-e118. https://doi.org/10.1128/MCB.00070-18

45. Moriyama, T., Yoneda, Y., Oka, M., Yamada, M. (2020). Transportin-2 plays a critical role in nucleo-cytoplasmic shuttling of oestrogen receptor-α. *Scientific Report*, 10(18640). https://doi.org/10.1038/s41598-020-75631-3.

46. Dubik, D., & Shiu, R. P. (1992). Mechanism of estrogen activation of c-myc oncogene expression. *Oncogene, 7*(8), 1587–1594.

47. Levin, E. R., & Hammes, S. R. (2016). Nuclear receptors outside the nucleus: Extranuclear signalling by steroid receptors. *Nature Reviews Molecular Cell Biology, 17*(12), 783–797. https://doi.org/10.1038/nrm.2016.122

48. Cavalcanti, F. N., Lucas, T. F., Lazari, M. F., & Porto, C. S. (2015). Estrogen receptor ESR1 mediates activation of ERK1/2, CREB, and ELK1 in the corpus of the epididymis. *Journal of Molecular Endocrinology, 54*(3), 339–349. https://doi.org/10.1530/jme-15-0086

49. Tecalco-Cruz, A. C., Perez-Alvarado, I. A., Ramirez-Jarquin, J. O., & Rocha-Zavaleta, L. (2017). Nucleo-cytoplasmic transport of estrogen receptor alpha in breast cancer cells. *Cellular Signalling, 34*, 121–132. https://doi.org/10.1016/j.cellsig.2017.03.011